Spectrochimica Acta Part A: Molecular and Biomolecular Spectroscopy 253 (2021) 119576

Contents lists available at ScienceDirect

Spectrochimica Acta Part A: Molecular and Biomolecular Spectroscopy

journal homepage: www.elsevier.com/locate/saa

Assessing the potential of para-donor and para-acceptor substituted 5-benzylidenebarbituric acid derivatives as push–pull electronic systems: Experimental and quantum chemical study

Ivana N. Stojiljković [a], Milica P. Rančić [a], Aleksandar D. Marinković [b], Ilija N. Cvijetić [c], Miloš K. Milčić [c,*]

[a] Faculty of Forestry, University of Belgrade, Kneza Višeslava 1, 11030 Belgrade, Serbia
[b] Faculty of Technology and Metallurgy, University of Belgrade, Karnegijeva 4, 11120 Belgrade, Serbia
[c] Faculty of Chemistry, University of Belgrade, Studentski trg 12-16, 11000 Belgrade, Serbia

HIGHLIGHTS

- 5-benyzlidenebarbiturates were investigated spectroscopically and theoretically.
- LFER analysis of spectral data and optimized geometry parameters are performed.
- ICT analysis for quantification of the efficiency of charge transfer is used.
- The best candidate for the push–pull system is *para*–$N(CH_3)_2$ substituted derivative.
- The weak electron-donating properties of barbituric acid are reported.

GRAPHICAL ABSTRACT

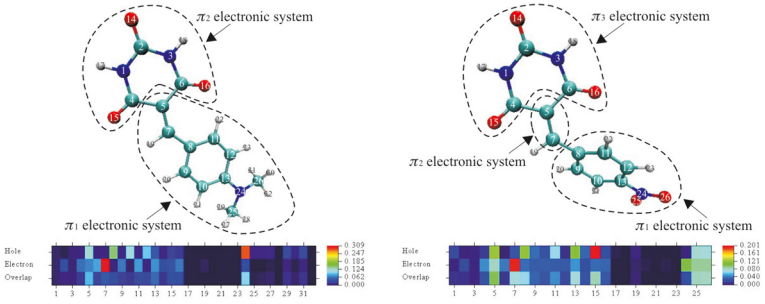

ARTICLE INFO

Article history:
Received 29 September 2020
Received in revised form 19 January 2021
Accepted 29 January 2021
Available online 13 February 2021

Keywords:
Barbituric acid derivatives
Push–pull systems
LFER analysis
ICT process
Hole-electron distribution analysis

ABSTRACT

Electronic interactions in donor-π-linker-acceptor systems with barbituric acid as an electron acceptor and possible electron donor were investigated to screen promising candidates with a push–pull character based on experimental and quantum chemical studies. The tautomeric properties of 5-benzylidenebarbituric acid derivatives were studied with NMR spectra, spectrophotometric determination of the p*K*a values, and quantum chemical calculations. Linear solvation energy relationships (LSER) and linear free energy relationships (LFER) were applied to the spectral data - UV frequencies and ^{13}C NMR chemical shifts. The experimental studies of the nature of the ground and excited state of investigated compounds were successfully interpreted using a computational chemistry approach including *ab initio* MP2 geometry optimization and time-dependent DFT calculations of excited states. Quantification of the push–pull character of barbituric acid derivatives was performed by the $^{13}CNMR$ chemical shift differences, Mayer π bond order analysis, hole-electron distribution analysis, and calculations of intramolecular charge transfer (ICT) indices. The results obtained show, that when coupled with a strong electron-donor, barbituric acid can act as the electron-acceptor in push–pull systems, and when coupled with a strong electron-acceptor, barbituric acid can act as the weak electron-donor.

1. Introduction

Barbituric acid and its synthetic derivatives are getting great attention from researchers due to their unique structural proper-

* Corresponding author.
E-mail address: mmilcic@chem.bg.ac.rs (M.K. Milčić).

https://doi.org/10.1016/j.saa.2021.119576
1386-1425/

ties and important technological and pharmaceutical applications. Various derivatives of barbituric acid were obtained by introducing the substituents in the C5 and N1/N3 positions of the barbituric acid ring, yielding compounds with a broad spectrum of biological activities such as antibacterial, antioxidant, as inhibitors of enzyme tyrosinase [1–3], and as selective oxidizing agents [4] for the synthesis of unsymmetrical disulfide [5,6]. Moreover, 5-ethylidenepyrimidine-2,4,6(*1H,3H,5H*) trione moiety has a broad range of applications in the design of dyes [7] and pigments [8] with multifunctional properties and as organic nonlinear optical materials [9,10].

Electron-donating substituent (D - push) covalently bonded to electron-accepting substituent (A - pull) via a π-conjugated bridge (linker) represent a class of molecules known as push–pull electronic systems (D-π-A). These compounds have attracted a great attention as organic materials with promising electronic and optical properties applied in non-linear optics (NLO) [11–14], dye-sensitized solar cells (DSSCs) [15,16], organic light-emitting diodes (OLEDs) [17], colorimetric pH sensors, and ions detection [18,19]. The structural motifs, important for the potential application of push–pull barbituric acid derivatives as NLO chromophores, are summarized in a brief article of *Ikeda et al* [20]. Some of the main features of push–pull systems are low energy intramolecular charge-transfer (ICT) band in absorption spectra, low HOMO-LUMO gap, and high value for first molecular hyperpolarizability. By varying three key elements (donor, π-linker, and acceptor) one can finely tune the HOMO-LUMO gap of the compound and modulate corresponding charge transfer interactions, which can influence its optoelectronic properties [21]. The computational chemistry methods of today can predict and explain the push–pull properties of a molecule. High level ground state quantum-chemical calculations can accurately predict the HOMO-LUMO gap, while time-dependent density functional theory (TDDFT) calculations of the excited state allow us to estimate the potential for the ICT transition in the various organic π-systems, as well as electronic properties of push–pull chromophores [22–25]. Also, based on the calculated electron density difference between ground and excited state charge-transfer distance (D_{CT}), which represents the distance between the location of the departing electron from the ground state and the locations of the arriving electron in the excited state, and the amount of charge transferred upon excitation (Q_{CT}) can be calculated [22].

The structure and properties of the barbituric acid moiety indicate that pseudoaromatic pyrimidine-2,4,6-trione ring can act as electron-donating or electron-accepting substituent in push–pull systems [26]. Electron-accepting abilities of barbituric acid moiety are well documented in the literature [7,27–30]. However, barbituric acid as electron-donor moiety in the molecules of the push–pull type is not yet confirmed [19,31–34].

In this study, a series of eleven 5-benzylidenebarbituric acid derivatives with different substituents were synthesized (Fig. 1) with the purpose of experimental and theoretical analysis on the nature of compounds and intermolecular interactions. Based on electron-donating/accepting properties the substituents can be roughly divided into four groups: *group I* is composed of strong electron-donors *i.e.* substituents with strong positive resonant effect (R) and weak negative inductive effect (I); *group II* contains weak electron-donors (alkyl substituents) with weak positive R and negligible I; in *group III* – (halogen group) are weak electron-acceptors, with large negative I and weak positive R and in *group IV* are strong electron-acceptor substituents with negative R and negative I. Also, an unsubstituted compound (compound **7**) was added for comparison purposes. A list of all substituents, together with their Hammett σ_{p+} parameters, as the good indicator of electron-donating/accepting ability, is shown in Fig. 1.

The nature of the ground and excited state of synthesized compounds were characterized and investigated using spectrochemical, solvatochromic (including LFER and LSER analysis), and computational chemistry approaches including optimization the molecular geometry, time-dependent DFT calculations of excited states, and the difference in charge distribution between the ground and excited state. Besides, the push–pull character of investigated molecules was quantified through parameters such as chemical shift differences, absorption spectra, HOMO-LUMO gap, hole-electron distribution analysis, and intramolecular charge transfer (ICT) analysis of excitations.

2. Experimental method

2.1. General method for synthesis of 5-benzylidenebarbituric acid derivatives

In this study, a series of substituted 5-benzylidenebarbituric acid derivatives were synthesized by Knoevenagel condensation [35,36] of barbituric acid with the corresponding benzaldehyde. 3 mmol of barbituric acid was dissolved in 20 ml hot distilled water and aromatic aldehyde (3 mmol) and 10 ml of 95% ethanol were added. The solution was stirred at room temperature between 0.5 h and 2 h, depending on the added aldehyde. The crude product was filtered off, purified by recrystallization from cold 95% ethanol, and dried. After the screening of different reaction conditions of Knoevenagel condensation, we found out that this was the most convenient way for the synthesis of *p*-substituted 5-benzylidene barbiturates.

2.2. Materials and methods

The chemical structure and purity of the synthesized compounds were confirmed by melting point, IR, ^{1}H and ^{13}C NMR, and elemental analysis. The melting points were determined on Stuart SMP10 digital melting point apparatus in an open capillary tube and are uncorrected. ^{1}H and ^{13}C NMR spectra were obtained using Varian 2000 spectrometer (200 MHz for ^{1}H and 50 MHz for ^{13}C) at room temperature in deuterated dimethyl sulfoxide (DMSO d_6) with TMS as the internal standard. Chemical shifts are reported in ppm (δ). IR spectra were recorded in Perkin Elmer FTIR-Spectrometer 1725X using the KBr pellet method. Microanalysis of carbon, hydrogen, and nitrogen was carried on an ElementarVario EL III. UV/Vis spectra were recorded in Shimadzu UV-1700 spectrophotometer using spectro-quality solvents at a fixed concentration sample of $1{\cdot}10^{-5}$ mol/dm^3. The UV/Vis spectra for pK_a values determination were recorded on Cintra 6 spectrophotometer (GBC Dandenong, Australia) with a 1 cm quartz cuvette in 220–700 nm range against the phosphate buffer as a blank. The pH values were measured with CRISON 50 29 micro-combined pH electrode (CRISON INSTRUMENTS, S.A. Spain). The electrode was calibrated by standard buffer solutions (pH 4.01, 7.00, and 9.21). The pK_a values for different tautomers of compound **1** were predicted using MarvinSketch software (https://chemaxon.com/products/marvin).

Qualitative estimation of the influence of the solvent on UV spectra was performed with a linear solvation energy relationship (LSER) analysis using the Kamlet-Taft solvatochromic equation [37]. This model separates non-specific (electrostatic effect - dipolarity/polarizability) and specific (hydrogen bond) solute-solvent interactions as given by Eg. (1):

$$\nu_{max} = \nu_o + s\pi* + b\beta + a\alpha \quad (1)$$

where ν_{max} is the absorption maxima shifts; ν_o is the regression value in cyclohexane as reference solvent; π^* is an index of the

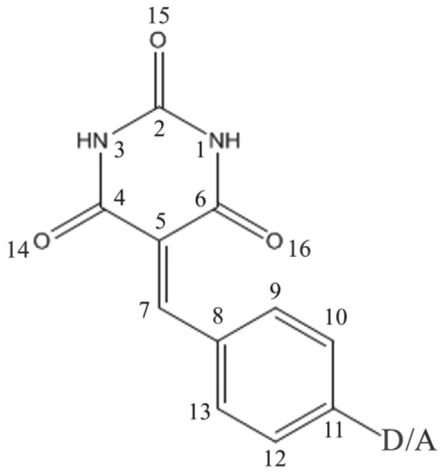

Compound	D/A	σ_{p+}
	Group I	
1	*p*-$N(CH_3)_2$	-1.7
2	*p*-OH	-0.92
3	*p*-OCH_3	-0.78
4	*p*-OCH_2CH_3	-0.81
	Group II	
5	*p*-CH_3	-0.31
6	*p*-$CH(CH_3)_2$	-0.28
7	**H**	0
	Group III	
8	*p*-F	-0.07
9	*p*-Cl	0.11
10	*p*-Br	0.15
	Group IV	
11	*p*-CN	0.66
12	*p*-NO_2	0.79

Fig. 1. Chemical structures of 5-benzylidenebarbituric acid derivatives including atom numbering and Hammett σ_{p+} values.

solvent dipolarity/polarizability; α is a measure of the solvent hydrogen-bond donor (HBD) acidity and β is a measure of the solvent hydrogen-bond acceptor (HBA) basicity. The Kamlet-Taft solvent parameters [37,38] π^*, β, and α are given in Table S1. The regression coefficients *s*, *b*, and *a* in Eq. (1) represent the individual contribution of solvatochromic effects on absorption frequencies.

The influence of substituent on the electron density distribution was studied by using a variety of linear free energy relationship (LFER) models [39,40]. For the correlation of NMR spectral data, the general form of one-parameter Hammett equation was initially used (S4) and then analyzed along with UV frequencies using two-parameter Hammett-Taft (extended Hammett Equation) and Swain-Lupton type correlations of substituent effects in their general form given by Eq. (S5) and (S6). Correlation analysis was performed using Microsoft Excel computer software at a confidence level of 95%. The correlation coefficient (*r*), the standard error of the estimate (*sd*), Fisher's significance test (*F*), and *t*-test (*t*) for individual regression coefficients were used as a measure of goodness of fit in regression analysis. All dependent variables were autoscaled between 0 and 1.

2.3. Characterization of 5-benzylidenebarbituric acid derivatives

^{1}H and ^{13}C NMR, IR, melting points, and elemental analysis data of compounds **1**–**12** are given in Supplementary material.

3. Computational methods

Optimal geometries of all investigated molecules were obtained by using the second-order Møller-Plesset (MP2) method [41] with the 6-311G(d,p) basis set. Absorption spectra were calculated using the TDDFT method, more specifically B3LYP functional which includes the Becke three-parameter exchange [42] and the Lee, Yang, and Parr correlation functionals [43] with a 6-311G(d,p) basis seton MP2/6-311G(d,p) optimized geometries. For absorption spectra calculations PCM (polarizable continuum model) implicit model of solvation effect was used for solvent simulation. The amount of charge transfer between the donor and acceptor was estimated as a difference between ground and excited state densities with charge-transfer indices (D_{CT} and Q_{CT}) [22]. The CT indices were calculated in acetonitrile solution (simulated with PCM method) with the method proposed by *Jacquemin et al* [23]. All the theoretical calculations were done in the quantum chemistry program Gaussian09 [44]. Mayer π bond order analysis of the nature of chemical bond [45], hole and electron distribution, conceptual DFT global reactivity descriptors and interfragment charge transfer analysis [46] was performed using Multiwfn 3.6 wavefunction analyzer [25] together with the Gaussian quantum chemical code.

4. Results and discussion

4.1. Isomerism of 5-benzylidenebarbituric acid derivatives

4.1.1. Experimental ^{1}H/^{13}C NMR study

5-Benzylidenebarbituric acid derivatives are structurally versatile compounds that might exist in several isomeric/tautomeric forms in solution (Fig. S1). The ^{1}H NMR spectra of compounds **1**–**12** found triketo form as the dominant tautomeric species in DMSO, as concluded by the presence of two –NH signals at ~11.3 ppm and the absence of signals of enolic –OH protons. Also, three distinct signals from carbonyl groups (165–163 ppm, 162.7–161.5 ppm, and 150 ppm) are found in ^{13}C NMR. These results corroborate previous studies on the isomerism of barbituric acid [47–49] as well as with crystal structures of benzylidenebarbituric acid compounds [50,51] deposited in the Cambridge Structural Database [52].

4.1.2. Spectrophotometric determination of the pKa values

To confirm the tautomeric preferences of 5-benzylidenebarbituric acid derivatives, we determined the pK_a values in aqueous solution for compound **1** bearing the strongest electron-donating substituent within the series. The macroscopic pK_a values are expected to depend on the tautomeric form of the compound and the pK_a for different tautomers predicted with MarvinSketch software for compound **1** are shown in Fig. S2. The changes in the ionization state of compound **1** were monitored at the absorption maxima around 255 nm (Figs. S3–S5).

Compound **1** is expected to show three ionization steps in the measurable pH range, two from barbituric acid moiety and one from protonated *N,N*-dimethylamino group at low pH values. Deprotonation of protonated *N,N*-dimethylamino group increases the electron density at the benzene ring chromophore. This reflects in the increased intensity of absorption peak at 255 nm (Fig. S3). Such a trend is continued at higher pH values where ionization of barbituric acid moiety occurs (Fig. S4). At even higher pH values, deprotonation of the third ionization center of compound **1**occurs and results in the decreased absorbance of the benzene ring chromophore (Fig. S5).

The absorption spectra of pure H_2A and HA^- were detected in the limited pH range where no further shift of the absorption spectra was observed as pH increased. The ionization constants of compound **1**, as well as the absorbances of H_3A^+ and A^{2-} forms, are obtained through the linearization of spectral data according to equations S1-S3 (Figs. S6–S8). Table 1 summarizes the pK_a values for compound **1**. According to pK_a predictions for three tautomeric forms (Fig. S2), a high pK_{a3} value (12.27 ± 0.02) indicates that triketo form is the main tautomeric form in solution (Fig. S2, left). It is reasonable to hypothesize that the other members of the congeneric series also exist as triketo tautomer in aqueous solution.

4.1.3. Quantum chemical study

Additionally, the MP2/6-311G(d,p) method was used for optimizing the geometry of all possible tautomers and determining their relative stability in the gas phase. The calculations confirm that the triketo forms are the most stable (Table S4). The diketo and monoketo tautomers are by 15.4–20.6 kcal/mol and 32.5–35. 8 kcal/mol, respectively, less stable than triketo tautomer (Table S4). The optimized structures of the most stable isomer of 5-benzylidenebarbituric acid derivatives from *ab-initio* calculations are depicted in Fig. S9.

4.2. Geometry optimization of 5-benzylidenebarbituric acid derivatives

A previous *ab initio* theoretical study examining the molecular structure and torsional profile of styrene found that the geometry of styrene is principally determined by the π – π interactions of the vinyl and phenyl groups and steric interactions [53]. The overestimation of the π-conjugation in DFT calculations leads to predictions of planar global minimum energy structure [54]. Other theoretical studies for this system [55,56] also confirmed that the results of the density functional theory calculations are in disagreement with the results from the Møller-Plesset second-order approximation. They concluded that the more conventional MP2 theory predicts much larger torsion angles, twisted styrene, and reasonably good agreement with the experimental results [57]. In addition to the above approach, geometries of all investigated compounds were fully optimized by minimizing the energies using the MP2 method with a 6-311G(d,p) basis set, and the nature of minima was confirmed by subsequent frequency calculations – no imaginary frequencies were found. We have shown that this method produced results that are in good agreement with experimental findings [58,59]. The results of these calculations are presented in Fig. S9 and Table 2.

Table 1
An overview of experimentally determined pK_as of compound 1.

	Compound 1	Ionization center
pK_{a1}	4.20 ± 0.02	*N,N*-dimethylamino group
pK_{a2}	7.88 ± 0.12	Barbituric acid amido NH
pK_{a3}	12.27 ± 0.02	Barbituric acid amido NH

Optimized geometries of all compounds are in nonplanar conformation and this is in agreement with the geometries of crystal structures of 3 keto tautomers of 5-benzylidenebarbituric acid derivatives found in the Cambridge Structural Database (CSD) (Fig. S10) [52]. The values of the dihedral angle θ, defined as the angle between planes containing benzene ring and barbituric acid moiety, are shown in Table 2.The large value for angle θ in unsubstituted compound **7** (42.4°) indicates a strong steric repulsion between carbonyl group from barbituric acid and *ortho*-hydrogen from the benzene ring, and a low amount of π-electron delocalization between two π- systems. Since the introduction of the substituent at C11 position will have no effect on the steric interactions, the changes in the dihedral angle θ can be a good indicator of the influence of the electronic effects of the substituent on the π-electron delocalization in the system.

The geometry of compound **1** is close to planar (θ = 4.4°) indicating a stronger delocalization of π- electrons across benzylidene moiety. Other compounds from the *group I* also have substantially lower values for angle θ (around 20°) than unsubstituted compound **7**, but the deviation from planarity is higher than for compound **1**. On the other side, compounds from *group IV* have a higher value of angle θ than unsubstituted compound due to the negative resonance effect of strong electron-accepting –CN and –NO_2 substituent.

4.2.1. Correlation between dihedral angles and Hammett and Swain-Lupton substituent constants

In order to differentiate between contributions of inductive (field) and resonance effects of the substituent to the angle θ, regression analysis according to the dual substituent parameter (DSP) Swain-Lupton model was done (equation S7). A good correlation is observed (r = 0.98). A small value for f (−0.02) indicates that the inductive (field) effect will not influence the value of a dihedral angle. On the other side, large and positive value for correlation coefficient r shows that the resonance effect of the substituent will be a dominant effect in determining the planarity of the molecule. Substituents with large electron-donating resonance effect (*group I*) will increase the delocalization of the electrons between the benzene ring and the double bond in the benzylidene fragment, resulting in the more planar geometry and lower values of angle θ. The opposite is true for compounds with –R effect (*group IV*), delocalization of π-electrons between the benzene ring and a double bond is decreased and the value for angle θ is higher than in unsubstituted compound. The same qualitative results are obtained with extended Hammett equation (S8) (results of the correlation are shown in SI).

4.3. LFER analysis of NMR data and Mayer π bond order analysis

In order to analyze the transfer of electronic effect of substituents through the molecules in their ground state, ^{13}C NMR data were fitted with Hammetťs mono substituent parameter (MSP) and extended Hammetťs and Swain-Luptońs dual substituent parameter (DSP) models. The results of ^{1}H and ^{13}CNMR spectroscopy showed that the chemical shifts are very sensitive to variable electron-donor and electron-acceptor substituents in benzylidene moiety. The values of substituent-induced chemical shifts (SCS) are shown in Table S5 as the difference between the chemical shift of unsubstituted compound **7** and the corresponding substituted derivative. As can be seen from Table S5, the high sensitivity of the ^{13}C NMR chemical shift to the local environment is observed for carbon atoms in the phenyl moiety of the molecules [60].

The substituents from *groups I*, *II*, and *III* increases π-electron density around the C_8 and C_{10} atoms, (average SCS values of −7.4 ppm and −14.8 ppm, respectively) and decrease π-electron

Table 2
The values of the dihedral angles for compounds **1**–**12** (in degrees) calculated at MP2 level.

Compound	1	2	3	4	5	6	7	8	9	10	11	12
Dihedral angle, θ(°)	4.4	19.6	20.7	20.0	39.1	39.0	42.4	38.3	39.6	40.2	44.8	44.4

density on C_9 atom (average chemical shift values of +4.6 ppm) due to positive resonance effect. In the case of substituents with negative resonance effect (compounds from *group IV*) the electron densities on C_8 atom are reduced causing an upfield shift of 4.8 and 7.0 ppm for compounds **11** and **12**. The chemical shift of C_9 atom is unaffected by electron-accepting substituent and there is a large upfield shift for C_{10} atom in compound **12**.

Much more interesting are SCS in C_7 and C_5 carbon atoms or C_α and C_β as often referred to in the literature [57,58,61,62]. The chemical shift of C_7 carbon atom are almost unaffected by substituents from *groups I* and *II* and shifted upfield for compounds from *groups III* and *IV*. The opposite behavior is observed for C_5, strong upfield shift for compounds from *groups I* and *II*, and downfield shift for compounds from *groups III* and *IV*.

In order to elucidate this, we investigated the distribution of π-electronic densities from B3LYP wavefunctions for ground states of compounds **1**–**12**. This distribution is shown in Fig. 2. Also, the results of the calculated Mayer π bond order for selected bonds are shown in Table 3.

Evident from the presented results is that the π bond order for the C_7-C_8 bond is decreasing (from 0.254 to 0.110) and the C_5-C_7 π bond order is increasing (from 0.545 to 0.704) with increasing electron-accepting capability of the substituent (Table 3). This is in line with the increasing deviation from planarity found in optimized geometries of investigated compounds, *i.e.* the lower the π bond order of the C_7-C_8 bond is, the higher is the angle between two planes. This practically means that the increase in electron-accepting capability of the substituent at the benzene ring will decrease the delocalization of π-electrons across the molecule. In the compounds from the *group I* (especially in compound **1**) there is a substantial amount of π-electron delocalization between benzene moiety and exocyclic C_5-C_7 bond (Fig. 2). This delocalization provides a resonant structure with the increased electron density at the C_5 carbon atom, causing a strong upfield SCS in ^{13}C NMR

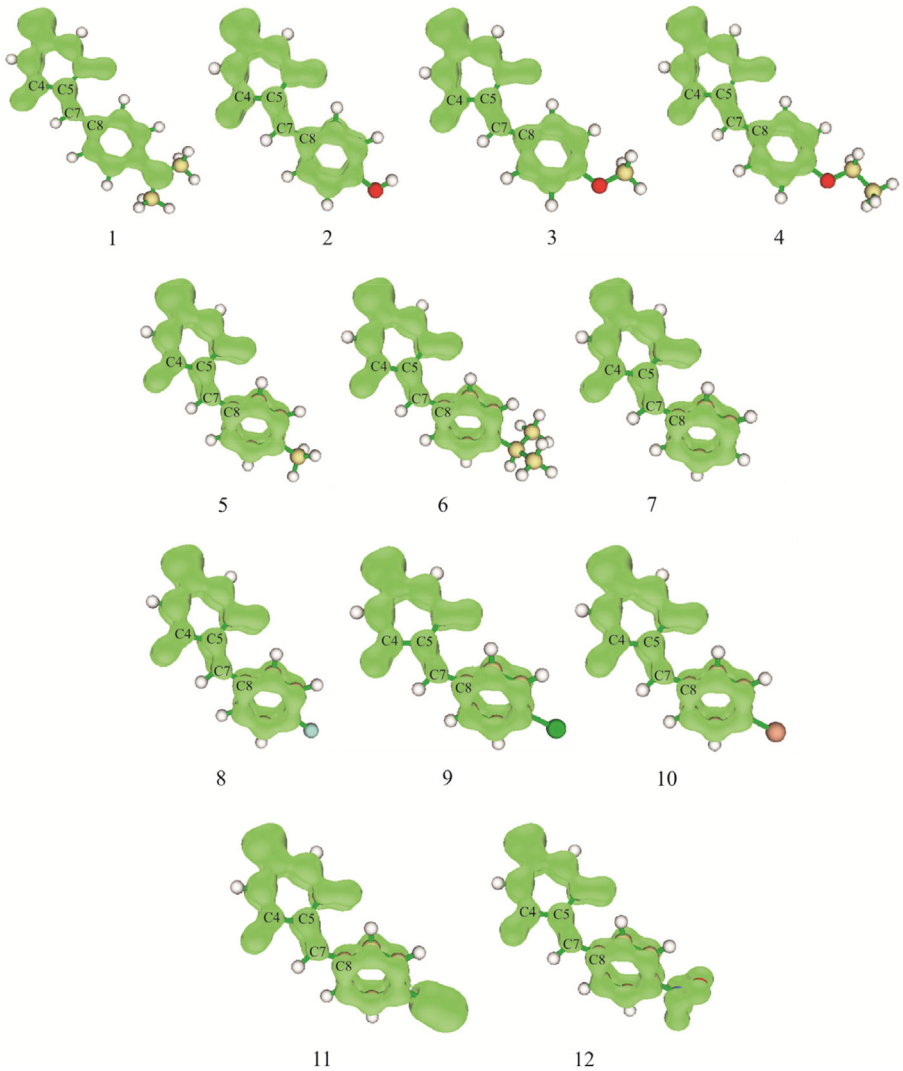

Fig. 2. Isosurface map (isosurface value = 0.027 au) of the distribution of π-electronic densities of compounds **1**–**12.**

Table 3
Mayer π bond orders for compounds **1-12.**

Bond	Bond order											
	1	**2**	**3**	**4**	**5**	**6**	**7**	**8**	**9**	**10**	**11**	**12**
C_4-C_5	0.130	0.118	0.118	0.118	0.109	0.109	0.105	0.107	0.105	0.104	0.097	0.096
C_5-C_7	0.545	0.597	0.597	0.596	0.649	0.650	0.669	0.656	0.667	0.669	0.700	0.704
C_7-C_8	0.254	0.209	0.209	0.210	0.158	0.158	0.140	0.154	0.145	0.143	0.113	0.110

spectra. For the compounds from *group IV* there is much less delocalization of π electronic density between benzene moiety and exocyclic C_5-C_7 bond (Mayer π bond order less than 50% of the bond order for a *group I*, Table 3), so the resonant effect have little influence on the SCS of C_5. The strong downfield shift for C_5 and upfield shift for C_7 can be attributed to the localized π-polarisation between the two π-systems (π_1 and π_2, Fig. 3). In a similar manner, the weak and downfield shift of the C_7 in the compound from the *group I* can be attributed to extended π-polarisation in the π_1-system of these compounds (Fig. 3).

Also, results of the Mayer π bond order analysis indicate that there is very little delocalization of π-electrons between barbituric acid moiety and the rest of the molecule, which is decreased when going from the *group I* to group *IV* (from 0.130 in compound **1** to 0.096 in compound **12**, Table 3). Based on the results of SCS from ^{13}C NMR spectra and the Mayer π bond order analysis indicating stronger delocalization of π-electrons between the benzene ring and vinyl group in compounds from the *group I*, we considered that these compounds will have only two π-systems (π_1 and π_2, Fig. 3a). On the other hand, compounds from *group II*, *III*, and *IV* will have three π-system (π_1, π_2, and π_3, Fig. 3b). This is further confirmed by very weak SCS on C_4 (an only compound from the *group I* have C_4 SCS larger than 1 ppm) and negligible SCS on C_2, Table S5.

To further analyze the substituent effect on ^{13}C chemical shifts of relevant carbon atoms (C_5, C_7, and C_8), linear models of Hammett and Swain-Lupton type were applied. The correlation results obtained by applying regression (LFER) models with literature substituent constants (σ_p, σ_p^+, σ_I, σ_{R+}, *F*, and *R+*) are given in Tables 4–6.

Better correlation with σ_p^+ electrophilic substituent constants for C_5 and C_8 (Table 4) atoms indicates a considerable contribution of extended resonance interaction in the overall electronic effect transmitted through π-units. Normal substituent effect ($\rho > 1$) is also noticed for C_5 and C_8. On the other hand, a negative sign for ρ values and better correlations results for C_7 atom in the case with σ_p substituent constants indicates a reverse trend.

From the DSP models (Tables 5 and 6), the positive sign of correlation coefficients for the C_8 and C_5 atoms and $\lambda > 1$ (resonance effect predominates over inductive/field effects) reflect normal substituent electronic effect while the negative values of ρ_I, ρ_R, *f*, and *r* for C_7, and $\lambda < 1$ indicate the reverse effect. The obtained results confirm the existence of a different mechanism of transmission of electronic substituent effects which includes localized and extended polarisation followed by extended π-resonance interaction, resulting in a change in molecular geometry.

4.3.1. The difference of chemical shift values, Δδ, as a measure of the push–pull character

Important properties of push–pull molecules are connected with differences between the chemical shifts ($\Delta\delta_{C=C}$) of two sp^2 carbon atoms which form an exocyclic double bond [63]. The indicators for the push–pull effect are high values of $\Delta\delta_{C=C}$ and C=C bond elongation. In case that the resonance effect is dominating, high values of $\Delta\delta_{C5=C7}$ are suited as direct measures of the push–pull effect. As can be seen in Table 7, the highest value of $\Delta\delta_{C5=C7}$ (44.34 ppm) for the strongest electron-donor substituent (compound **1**) indicated a higher degree of resonance. On the contrary, electron-accepting groups cause a decrease in $\Delta\delta_{C5=C7}$ and the lower degree of π-electron delocalization, which is confirmed by the small value of $\Delta\delta_{C5=C7}$ (28.81 ppm) for compound **12**. Based on the obtained results, compound **1** is the best candidate for the push–pull system and further study in unraveling the existence of the intramolecular charge transfer (ICT) process.

4.4. Absorption spectra of 5-benzylidene barbiturates in different solvents

It is well known that the position of absorption maximum depends on the chemical and physical properties of certain solvent as a result of appropriate electronic transition which directly depends on chromophores and type of electron transition. The

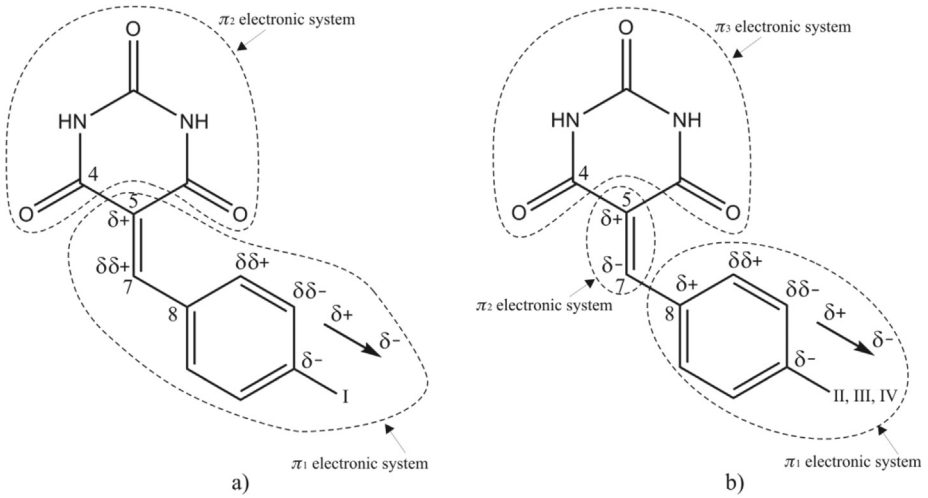

Fig. 3. Compounds from the groups I, II, III, and IV with the contribution of (a) localized π-polarisation and (b) extended π-polarisation.

Table 4
Correlation results of 13C SCS values with the Hammett substituent constants σ_p and σ_p^+.

Atom		*ρ*	*h*	*r*	*sd*	*t*	*F*
C_5	**σ_p**	2.18 ± 0.19	0.01 ± 0.08	0.97	0.27	11.72	137.38
	σ_p^+	**1.42 ± 0.03**	**0.37 ± 0.02**	**1.00**	**0.08**	**42.71**	**1824.16**
C_7	**σ_p**	**−2.12 ± 0.24**	**−0.01 ± 0.10**	**0.94**	**0.36**	**−8.69**	**75.59**
	σ_p^+	−1.24 ± 0.22	−0.33 ± 0.16	0.87	0.51	−5.64	31.80
C_8	**σ_p**	2.16 ± 0.21	0.01 ± 0.09	0.96	0.31	10.37	107.60
	σ_p^+	**1.39 ± 0.09**	**0.37 ± 0.07**	**0.98**	**0.22**	**14.64**	**214.44**

$t_{kr(\alpha=0.05,\ \nu=9)}$ = 2.26; $F_{kr(\alpha=0.05,\ \nu=1,\ \nu=9)}$ = 4.96.

Table 5
Correlation results of 13C SCS values withσ_I and σ_{R+}.

Atom	ρ_I	ρ_R	*r*	*sd*	^{I}t	^{R}t	*F*	*ρR/ρF*
C_5	1.17 ± 0.14	2.19 ± 0.09	1.00	0.11	8.07	25.47	479.42	1.87
C_7	−2.75 ± 0.54	−1.23 ± 0.32	0.93	0.40	−5.12	−3.83	30.44	0.45
C_8	0.83 ± 0.36	2.23 ± 0.22	0.97	0.27	−2.27	10.34	71.93	2.69

$^{I,R,f,r}t_{kr(\alpha=0.05,\ \nu=9)}$ = 2.26; $^{d}F_{kr(\alpha=0.05,\ \nu=2,\ \nu=9)}$ = 4.31.

Table 6
Correlation results of 13C SCS values with F and R+.

Atom	*f*	*r*	*r*	*sd*	^{f}t	^{r}t	*F*	*λ(r/f)*
C_5	1.36 ± 0.12	1.43 ± 0.04	1.00	0.08	11.47	35.25	845.19	1.05
C_7	−3.12 ± 0.45	−0.89 ± 0.15	0.96	0.31	−6.89	−5.73	53.70	0.29
C_8	1.10 ± 0.33	1.44 ± 0.11	0.98	0.22	3.34	12.88	106.36	1.31

^{I,R,f,r} $t_{kr(\alpha=0.05,\ \nu=9)}$ = 2.26; $^{d}F_{kr(\alpha=0.05,\ \nu=2,\ \nu=9)}$ = 4.31.

Table 7
Selected chemical shift values of the carbon atoms (δ, ppm) and chemical shift differences ($\Delta\delta_{C5=C7}$).

Compound	**1**	**2**	**3**	**4**	**5**	**6**	**7**	**8**	**9**	**10**	**11**	**12**
δ_{C5}	111.46	115.84	115.78	115.64	118.19	118.12	119.38	118.98	119.97	120.07	122.16	122.64
δ_{C7}	155.80	155.90	155.29	155.31	155.26	155.30	155.01	153.78	153.32	153.39	152.02	151.45
$\Delta\delta_{C5=C7}$	44.34	40.06	39.51	39.67	37.07	37.18	35.63	34.8	33.35	33.32	29.86	28.81

term solvatochromism was used to describe the change of the position of UV/Vis absorption band depending on dipolarity/polarizability and proton or electron transfer between solvent and solution, enabling assessment of basic properties of molecules [64]. Generally, the planarity of molecules and the size of delocalized π-electron systems have a decisive influence on the shape and wavelength position of the UV/Vis spectra of a certain molecule. Positive solvatochromism, appropriate bathochromic (red) shift, was connected with increased planarity which facilitates π-electron delocalization.

In order to analyze the effect of solvents, the absorption spectra of the investigated compounds were recorded in 21 solvents with different properties (polarity, HBA, and HBD ability), in the wavelength range from 200 to 800 nm. The spectra show two absorption maxima in the range of 230–480 nm. The lowest-energy maximum at 310–480 nm and the second high-energy maximum at 230–260 nm can be observed in the considered solvents. Since every solvent has a UV absorbance cut-off wavelength, the second absorption maximum, due to the absorption of some solvent in that spectrum region, could not be registered in all the solvents, so only the first absorption band was taken for further analysis. The part of recorded UV spectra (280–600 nm) of all investigated compounds in methanol, acetonitrile, THF, and chloroform are presented in Fig. 4. Table S6 contains absorption frequencies for the first absorption band for all solvents.

The results clearly indicate that the values of the maximum absorption frequencies, ν_{max}, depends more on the nature of the substituents than on the nature of the solvents. Generally, the values of the maximum absorption frequencies, ν_{max}, show that the substituents on the phenyl ring of 5-benzylidenebarbituric acid derivatives cause a bathochromic shift in relation to the unsubstituted compound **7** in all solvents for compounds from *groups I*, *II*, and *III*. Compounds from *group IV* are hypsochromically shifted relative to the unsubstituted compound. The different behavior of these compounds may be explained by the negative resonance effect of the strong electron-acceptors (–CN and $–NO_2$) in contrast to the positive resonance effect of substituents in compounds from other groups. Large positive resonance effect of substituents from a *group I* induces the largest bathochromic shift. This shift is the most pronounced in compound **1** because -NMe_2 substituent has the strongest resonance effect of all substituents (Table S6). Substituents in compounds from *group II* and *III* have similar, weakly positive resonance effect, but compounds from *group III* are less bathochromiaclly shifted because of large negative inductive effect from their substituents. The influence of negative inductive effect on the absorption band shift is the most visible in compounds from *group III*; compound **10** is more bathochromcally shifted than compounds **8** and **9** because -Br substituent has a weaker negative inductive effect than -F and -Cl substituents. Compound **8** with fluorine substituent with strongest negative I is less bathochromically shifted then compounds **9** and **10**.

4.5. Solvent effects on the UV/Vis absorption spectra - LSER analysis

From Fig. 4 it is obvious that the position of the first absorption band of investigated compounds is very weakly influenced by the

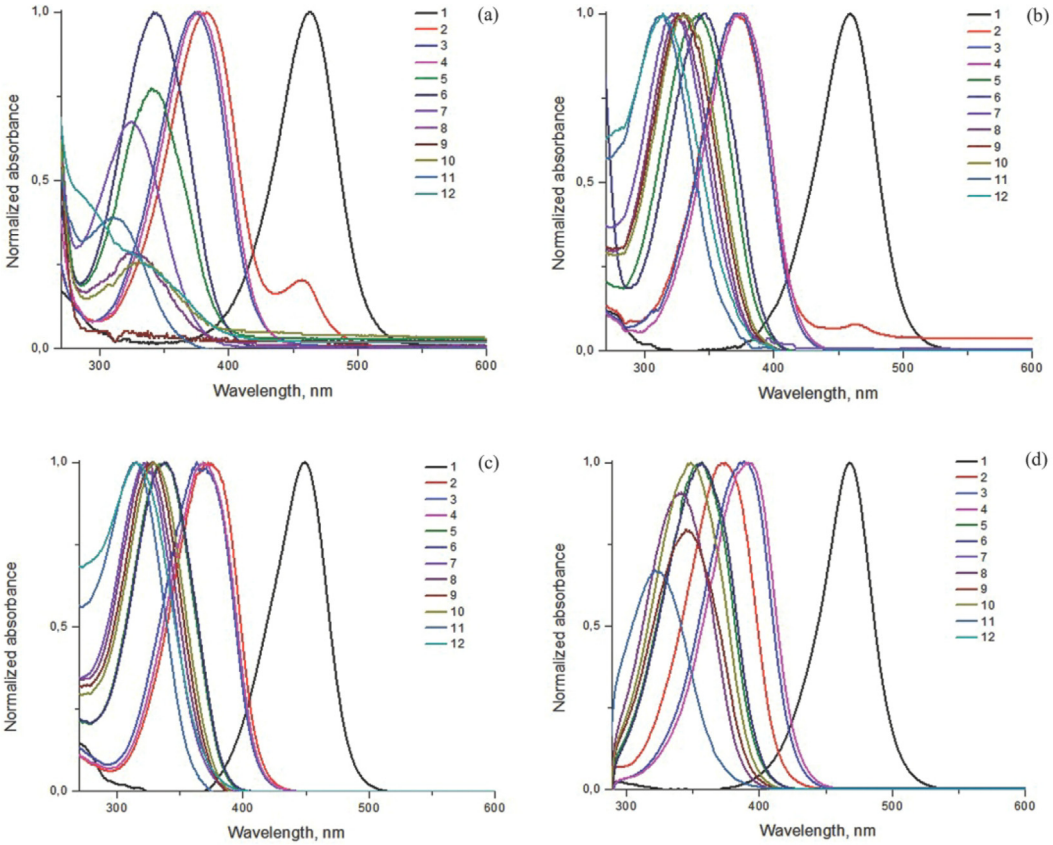

Fig. 4. Absorption spectra of compounds **1**–**12** in MeOH (a), MeCN (b), THF (c), and TCM (d).

solvent, *i.e.* that the investigated compounds are weakly solvatochromic. Nevertheless, the effect of the solvent on the absorption spectra of 5-benzylidenebarbituric acid derivatives was tested by LSER analysis using the Kamlet-Taft solvent parameter sets. In our research, 10 alcoholic solvents (fluorinated, mono- and polyhydroxy) and 11 aprotic solvents are selected for investigating the position of the visible UV/Vis absorption band. In the case of alcoholic solvents the Kamlet-Taft model including KAT solvatochromic parameters is the most suitable solvatochromic method for the interpretation of the solvent polarity effects on the absorption spectra [65]. The values of solvatochromic coefficients *s*, *b*, and *a* are listed in Tables S7. The presented results confirm that the solvatochromic effects observed in UV/Vis spectra of **1**–**12** are complex due to the interplay of both solvent and substituent effects.

Results of Kamlet-Taft analysis show that compounds with substituents with positive R (compounds from *groups I* and *II*) have a negative sign of coefficient *s* indicating that increase of solvent dipolarity/polarizability will increase the bathochromic shift of the first absorption band. This effect is most pronounced for compounds from the *group I* especially for compound **1** with strong electron-donating -NMe_2 substituent. This might be explained by better solvation stabilization of the excited state relative to the ground state. These results indicate that the excited state is more polar and polarizabile compared with the ground state [21]. The effect of solvent dipolarity/polarizability on compounds from *group III* and *IV* is much weaker which is confirmed by negligible values of regression coefficient *s* with high standard errors. A negative sign of the coefficient *a* for all compounds (Table S7), except for compound **11,** indicates a bathochromic (red) shift with an increase in the hydrogen-bond donor (HBD) capabilities of the solvent. This indicates better stabilization of the excited state relative to the ground state with increasing solvent acidity. Compound **11** is excluded from this analysis due to statistically insignificant results. The highest absolute value~~s~~ of coefficient *a* was found for compound **12**.

The positive sign of the coefficient *b* for most compounds, except for compound **12**, reflects hypsochromic (blue) shift with an increase of hydrogen-bond accepting (HBA) ability of the solvent (Table S7). High positive values of the coefficient *b* indicate higher contribution of solvent acidity to the ground state stabilization. In this case, compounds **1** and **2** are excluded from the analysis (statistically insignificant results). Compound **12** is the exception from this trend, negative and larger absolute value of coefficient *b* indicates bathochromic (red) shift with increasing solvent basicity (HBA). It can be noticed, from the results given in Table S7, that in most cases λ_{max} are more sensitive to the effects of hydrogen bond acceptor ability of solvents. The obtained results for coefficient *b* indicate that the *nitro* substituted derivative is more susceptible to the solvent HBA stabilization in the excited state. It could be postulated that the different behavior of compound **12** is a consequence of the existence of π_3-electronic system and the different conjugational ability of the π-electron densities through localized π-unit (π_1-, π_2-, and π_3-) in the presence of the NO_2 group. This suggested that the introduction of the strong electron-accepting substituents can lead to an increased proton-donating ability of the NH group of barbituric acid.

On the other hand, the solvatochromic behavior of the enol form of a *nitro* substituted barbiturates in solvents of different polarity are well documented in the literature [19,31,33]. The enol form of a *nitro* substituted derivatives of barbituric acid shows a bathochromic shift in the UV/Vis absorption bands with increasing

solvent hydrogen-bond accepting capability. [19,31] The findings indicate that the enol tautomer is stabilized by hydrogen bonds between the enol OH group and solvent [19,31,33]. With this in mind, it is possible that the presence of some amount of mono-enol tautomeric form in solution of a *nitro* substituted derivative **12** will cause a bathochromic shift (and a negative sign of coefficient *b*) with increasing the solvent basicity. Based on this, broadening and splitting of the first absorption band for compound **12** found in some of the considered solvents (Fig. S11) can originate from keto-enol tautomerization of barbituric acid part of molecule and specific solvent–solute interaction realized through hydrogen bonding. In general, the effect of the solvent on the UV absorption spectra of the investigated compounds is very complex and the results suggest that there is a correlation between the potential candidates for the push–pull or pull–push structure and the position of absorption maxima in the solvents of different polarity.

4.6. Substituent effects on the UV spectra- LFER analysis

To investigate the transmission of substituents effects in compounds **1**–**12**, extended Hammett's equation (S5) was applied for correlating light absorption properties. Based on the correlation between the σ_I and σ_R substituent constants and the UV/Vis spectral data (Table S8), a significantly stronger contribution of resonance substituent effect relative to inductive/field effect is observed (ratio of $\rho R/\rho I$ = 2.50–5.00 and r value between 0.95 and 0.98) in all solvents. Generally, the electronic effects are transmitted through the molecule in the same manner in all solvents, as confirmed by the positive value of the proportionality constant, ρ.

4.7. ICT process and evaluation of push–pull chromophores

In order to further elucidate the nature of absorption spectra, TDDFT calculations for all investigated compounds in solvent acetonitrile were done and the results are shown in Table S9. Since our goal was to investigate the nature of lowest energy absorption maxima found in experimental spectra (between 310 and 480 nm, *i.e.* 4.00–2.58 eV) results are shown only for excitations with wavelengths higher than 290 nm (4.28 eV) and oscillator strength larger than 0.05. The results of TDDFT calculations (Fig. S12) are in good qualitative agreement with experimental spectra; compounds from a *group I* have the strongest bathochromic shift compared to unsubstituted compound, the compounds from *groups II* and *III* are slightly bathochromically shifted and absorption maxima for compounds from *group IV* are at the same wavelength as the unsubstituted compound (slightly hipsochromically shifted in experimental spectra). TDDFT calculations were also able to correctly predict the influence of negative inductive effect on absorption band in compounds from *group III* (Fig. S12-c); compound **10** with -Br substituent (weaker –I effect) is more bathochromically shifted than compounds with -Cl and -F substituent (stronger –I effect).

For compounds from a *group I* there is only one excitation in the selected energy range and it can be characterized as the simple HOMO → LUMO transition with more than 95% contribution from this orbital transition (Table S9). Compounds from *groups II* and *III* and unsubstituted compound **7** have two excitations in the selected energy range with similar oscillator strengths and energy difference from 21 to 26 nm so the lowest energy absorption maxima observed in experimental spectra will be the superposition of these two excitations (Fig. S12, b and c). The first excitation in these compounds is dominated by HOMO → LUMO transition (from 55% to 75% contribution) with an admixture of HOMO-1 → LUMO (from 13% to 34%). This can be explained with smaller HOMO to HOMO-1 gap in these compounds (from 0.30 eV to 0.61 eV) when compared to compounds from the *group I* (from 0.90 eV to 1.47 eV) (Fig. S13). The same orbital transitions are found in the second excitations with a small admixture of HOMO-2 → LUMO transition with contributions from 14% to 23%. The lowest energy absorption maxima for compounds from *group IV* is composed of three excitations with the second excitation having the highest oscillator strength (Table S9, Fig. S12-d). The dominant transition in this excitation is HOMO-1 → LUMO (49.03% and 40.20%), followed by HOMO → LUMO (34.16% and 31.64%) and HOMO-2 → LUMO (12.10% and 12.14%) transitions.

From MO energies shown in Fig. S13, it is obvious that the energy of the LUMO orbital remains almost unaltered in compounds from *groups I*, *II*, and *III* when compared to compound **7**. As expected, when strong electron-acceptors are introduced in compounds from *group IV* the energy of the LUMO is significantly lowered by 0.33 eV for compound **11** and 0.57 eV for compound **12**. On the other side, the strongest electron-donor –NMe_2 substituent in compound **1** will raise the energy of HOMO by 1.1 eV. Other (weaker) electron-donating substituents from the *group I* will also raise the energy of HOMO but by a lesser amount (from 0.44 eV to 0.51 eV). As a consequence, the HOMO-LUMO gap in compounds from the *group I* will be significantly lower, resulting in bathochromically shifted adsorption spectra [28,66] and higher value of electronic chemical potential (μ) (Table S10). As expected, compounds from *group IV* will have lowest value of electronic chemical potential (highest electronegativity) and highest value of global electrophilicity index (ω) (Table S10) since they have a strong electron-accepting groups in their structure. On the other hand, compound **1**, with strong electron-donating substituent will be the strongest nucleophile, with highest nucleophilicity index (N) among investigated compounds (Table S10) [67,68].

The intramolecular charge transfer (ICT) process occurs during the absorption of a photon by the excitation of molecules when electron density is shifted from one moiety of a molecule to another one. The electron density difference between the ground and the excited state has been used to quantify the efficiency of charge transfer in potential push–pull chromophores. ICT indices *i.e.* charge-transfer distance (D_{CT}) which represents the distance between two barycenters and the amount of transferred charge (Q_{CT}) for all investigated compounds were calculated and results are presented in the last two columns of Tables S9 and in Fig. S14. Based on TDDFT results obtained, it can be seen that the strongest ICT occurs in compounds from the *group I* (D_{CT} from 4.20 to 3.05 Å) with the strongest electron-donating substituents.

For example, in the compound **1**, upon excitation,electronic density is shifted across the longest distances (4.20 Å), from the electron-donating -NMe_2 substituent to the C_7 atom in the vinyl group and carbon atoms from the pyrimidine ring of barbituric acid. This was confirmed by the hole-electron distribution analysis of the first excitation of compound **1** (Fig. S15-a). In this excitation, 28% of the hole is located on the nitrogen atom from -NMe_2 substituent and 40% of the electron is located on barbituric acid moiety. The rest of the electron is located on the C_7 atom (30%). Also, carbon atoms from the benzene ring contribute substantially to the hole (42%). Generally, as in the typical push–pull system, excitation in compound **1** can be described as electron transfer from -NMe_2 substituent and benzene ring as electron-donors to the C_7 vinyl atom and barbituric acid as electron-acceptors. Similar conclusions can be drawn for other compounds from *group I*. Compounds from *groups II* and *III* have two excitations and none of them can be described as ICT excitation (Fig. S14). In these compounds, some amount of electron density is transferred from benzene ring carbon atoms to the C_7 atom from the vinyl group. Also, upon excitation there is a noticeable rearrangement of electron density in barbituric acid; electron density is transferred from oxygen atoms to the carbon atoms from the same carbonyl group (Fig. S14).

A reverse direction of ICT is observed in the first two excitations of compound **12**. Here a positive barycenter (representing a center of the charge loss) is located close to barbituric acid and a negative barycenter (representing center of the charge gain) is at benzene ring with $-NO_2$ substituent. This implies that, upon excitation, there is some charge transfer from barbituric acid as an electron-donor to $-NO_2$ substituent as an electron-acceptor. This was further confirmed with hole-electron distribution analysis (Fig. S15-b). In the first excitation, the hole is mostly located at barbituric acid oxygen atoms (60%) and the electron is mainly located at C_7 atom (25%) and a smaller amount at $-NO_2$ group (14%). ICT from barbituric acid to NO_2 is also noticed in the second excitation; 45% of the hole is located at barbituric acid moiety and 30% of the electron is located at $-NO_2$ group. Interfragment charge transfer (IFCT) analysis [25] can be a valuable tool to quantitatively describe electron redistribution between fragments during the excitation [69]. The results of IFCT analysis show that a total of 0.11 electrons are transferred from barbituric acid moiety to $-NO_2$ substituent in the first excitation and 0.08 electrons are transferred from barbituric acid moiety to $-NO_2$ substituent in the second excitation. These results clearly point out that, when coupled with the strong electron-accepting chromophore barbituric acid can act as a very weak electron-donating group. This observation shows that in all chromophores investigated, except compound **1**, some extent degree of charge transfer occurs, but they are not promising candidates for push–pull systems and cannot be used as typical CT compounds.

5. Conclusion

A systematic experimental and theoretical investigation of electron interactions in different substituted 5-benzylidenebarbituric acid derivatives has been done. The tautomeric preferences of investigated compounds have been studied by NMR spectra, spectrophotometric determination of the p*K*a, and quantum chemical calculations, and our results confirm that the most stable tautomer of the barbituric acid moiety is the triketo form.

MP2 optimizations suggest that the most stable keto isomers of 5-benzylidenebarbituric acid derivatives are generally nonplanar structures except derivatives bearing strong electron-donating substituents. The geometry of compound **1** containing strong electron-donor substituent is close to planar (θ = 4.4°) indicating a stronger delocalization of π-electrons across benzylidene moiety.

The results of LSER analysis showed that the shape and wavelength position of the UV/Vis spectra are more substituent-dependent than solvent-dependent. The Hammett SSP and Swain Lupton DSP models of ^{13}C NMR chemical shift indicate that polar and resonance effects of substituent operate at the C_8 and C_5 atoms and a reverse effect at C_7.

A quantitative description of the chemical bond (π bond order for C_4-C_5 and C_4-C_5) shows that an increase in electron-accepting capability of the substituent at the benzene ring will decrease the delocalization of π-electrons across the molecule. The results of the π bond order for C_4-C_5 indicate a low extent of π-electrons delocalization between barbituric acid moiety and the rest of the molecule.

In the compound from the *group I* there is a substantial extent of π-electron delocalization between benzene moiety and exocyclic C_5-C_7 double bond and the much less delocalization for the compound from *group IV*. Based on the results of SCS from ^{13}C NMR spectra and the Mayer π bond order analysis have been observed that the compounds from the *group I* have two π-systems and compounds from *group II*, *III*, and *IV* three π-systems.

Results of TDDFT calculations and ICT analysis applied on excited-state electron density for quantification of the efficiency of charge transfer in potential push–pull chromophores indicates that the strongest ICT occurs in compounds with the strongest electron-donating substituents (D_{CT} from 4.20 to 3.05 Å).

The results obtained from the analysis of excitations show, that when coupled with a strong electron-donor, barbituric acid can act as the electron-acceptor and when coupled with a strong electron-acceptor, barbituric acid can act as the weak electron-donor.

These studies clearly show that compound **1** can be considered as the best candidate for a push–pull system. It means that excitation in compound **1** can be described as electron transfer from -NMe_2 substituent and benzene ring as electron-donors to the C_7 vinyl atom and barbituric acid as electron-acceptors. Other chromophores investigated do not possess push–pull character and cannot be used as typical CT compounds.

CRediT authorship contribution statement

Ivana N. Stojiljkovic: Investigation, Writing - original draft, Writing - review & editing, Formal analysis, Project administration. **Milica P. Rančić:** Conceptualization, Validation. **Aleksandar D. Marinković:** Supervision, Resources, Funding acquisition. **Ilija N. Cvijetić:** Investigation, Formal analysis. **Miloš K. Milčić:** Conceptualization, Methodology, Writing - original draft, Writing - review & editing, Supervision, Funding acquisition.

Declaration of Competing Interest

The authors declare that they have no known competing financial interests or personal relationships that could have appeared to influence the work reported in this paper.

Acknowledgement

This work was supported by the Ministry of Education, Science and Technological Development of Republic of Serbia (Contract number: 451-03-9/2021-14/200168).

Appendix A. Supplementary material

Supplementary data to this article can be found online at https://doi.org/10.1016/j.saa.2021.119576.

References

[1] Q. Yan, R. Cao, W. Yi, Z. Chen, H. Wen, L. Ma, H. Song, Inhibitory effects of 5-benzylidene barbiturate derivatives on mushroom tyrosinase and their antibacterial activities, Eur. J. Med. Chem. 44 (2009) 4235–4243, https://doi.org/10.1016/j.ejmech.2009.05.023.

[2] M.K. Haldar, M.D. Scott, N. Sule, D.K. Srivastava, S. Mallik, Synthesis of barbiturate-based methionine aminopeptidase-1 inhibitors, Bioorg. Med. Chem. Lett. 18 (2008) 2373–2376, https://doi.org/10.1016/j.bmcl.2008.02.066.

[3] M.K. Khalid, A. Muhammad, A. Asma, P. Shahnaz, M.I. Choudhary, R. Atta ur, Synthesis of 5-arylidene barbiturates: a novel class of DPPH radical scavengers, Lett. Drug Des. Discov. 5 (2008) 286–291, https://doi.org/10.2174/157018008784619889.

[4] K. Tanaka, X. Cheng, T. Kimura, F. Yoneda, Mild oxidation of allylic and benzylic alcohols with 5-arylidene barbituric acid derivatives as a model of redox coenzymes, Chem. Pharm. Bull. (Tokyo) 34 (1986) 3945–3948, https://doi.org/10.1248/cpb.34.3945.

[5] K. Tanaka, X. Chen, T. Kimura, F. Yoneda, Oxidation of thiol by 5-arylidene 1,3-dimethylbarbituric acid and its application to synthesis of unsymmetrical disulfide, Tetrahedron Lett. 28 (1987) 4173–4176, https://doi.org/10.1016/S0040-4039(00)95570-9.

[6] K. Tanaka, X. Chen, F. Yoneda, Oxidation of thiol with 5-arylidene-1,3-dimethylbarbituric acid: application to synthesis of unsymmetrical disulfide1, Tetrahedron. 44 (1988) 3241–3249, https://doi.org/10.1016/S0040-4020(01)85957-3.

[7] M.C. Rezende, P. Campodonico, E. Abuin, J. Kossanyi, Merocyanine-type dyes from barbituric acid derivatives, Spectrochim. Acta Part A Mol. Biomol. Spectrosc. 57 (2001) 1183–1190, https://doi.org/10.1016/S1386-1425(00)00461-3.

[8] D. Thetford, A.P. Chorlton, J. Hardman, Synthesis and properties of some polycyclic barbiturate pigments, Dye. Pigment. 59 (2003) 185–191, https://doi.org/10.1016/S0143-7208(03)00104-9.
[9] K. Kondo, S. Ochiai, K. Takemoto, M. Irie, Nonlinear optical properties of p-substituted benzalbarbituric acids, Appl. Phys. Lett. 56 (1990) 718, https://doi.org/10.1063/1.102691.
[10] F. Kajzar, Organic Thin Films for Waveguiding Nonlinear Optics, CRC Press, 1996.
[11] G.S. He, L.S. Tan, Q. Zheng, P.N. Prasad, Multiphoton absorbing materials: molecular designs, characterizations, and applications, Chem. Rev. 108 (2008) 1245–1330, https://doi.org/10.1021/cr050054x.
[12] Y. Kawabe, H. Ikeda, T. Sakai, K. Kawasaki, Second-order non-linear optical properties of new organic conjugated molecules, J. Mater. Chem. 2 (1992) 1025–1031, https://doi.org/10.1039/jm9920201025.
[13] S.R. Marder, J.W. Perry, Molecular materials for second-order nonlinear optical applications, Adv. Mater. 5 (1993) 804–815, https://doi.org/10.1002/adma.19930051104.
[14] J. Podlesný, O. Pytela, M. Klikar, V. Jelínková, I.V. Kityk, K. Ozga, J. Jedryka, M. Rudysh, F. Bureš, Small isomeric push-pull chromophores based on thienothiophenes with tunable optical (non)linearities, Org. Biomol. Chem. 17 (2019) 3623–3634, https://doi.org/10.1039/c9ob00487d.
[15] A. Hagfeldt, G. Boschloo, L. Sun, L. Kloo, H. Pettersson, Dye-sensitized solar cells, Chem. Rev. 110 (2010) 6595–6663, https://doi.org/10.1021/cr900356p.
[16] Y. Wu, W. Zhu, Organic sensitizers from D–π–A to D-A–π–A: effect of the internal electron-withdrawing units on molecular absorption{,} energy levels and photovoltaic performances, Chem. Soc. Rev. 42 (2013) 2039–2058, https://doi.org/10.1039/C2CS35346F.
[17] Y. Ohmori, Development of organic light-emitting diodes for electro-optical integrated devices, Laser Photon. Rev. 4 (2010) 300–310, https://doi.org/10.1002/lpor.200810059.
[18] Y.H. Kim, H. Kim, H.J. Kim, Synthesis and pH-sensing properties of a push-pull conjugated fluorophore based on dicyanomethylene-1,4-dihydropyridine, Bull. Korean Chem. Soc. 37 (2016) 494–499, https://doi.org/10.1002/bkcs.10711.
[19] I. Bolz, M. Bauer, A. Rollberg, S. Spange, Chromophoric barbituric acid derivatives with adjustable hydrogen-bonding patterns as component for supramolecular structures, Macromol. Symp. 287 (2010) 8–15, https://doi.org/10.1002/masy.201050102.
[20] H. Ikeda, Y. Kawabe, T. Sakai, K. Kawasaki, Second order hyperpolarizabilities of barbituric acid derivatives, Chem. Lett. 18 (1989) 1803–1806, https://doi.org/10.1246/cl.1989.1803.
[21] F. Bureš, Fundamental aspects of property tuning in push-pull molecules, RSC Adv. 4 (2014) 58826–58851, https://doi.org/10.1039/c4ra11264d.
[22] T. Le Bahers, C. Adamo, I. Ciofini, A qualitative index of spatial extent in charge-transfer excitations, J. Chem. Theory Comput. 7 (n.d.) 2498–2506. https://doi.org/10.1021/ct200308m.
[23] D. Jacquemin, T. Le Bahers, C. Adamo, I. Ciofini, What is the "best" atomic charge model to describe through-space charge-transfer excitations?, Phys Chem. Chem. Phys. 14 (2012) 5383, https://doi.org/10.1039/c2cp40261k.
[24] I. Ciofini, T. Le Bahers, C. Adamo, F. Odobel, D. Jacquemin, Through-space charge transfer in rod-like molecules: lessons from theory, J. Phys. Chem. C. 116 (n.d.) 11946–11955. https://doi.org/10.1021/jp3030667.
[25] T. Lu, F. Chen, Multiwfn: a multifunctional wavefunction analyzer, J. Comput. Chem. 33 (2012) 580–592, https://doi.org/10.1002/jcc.22885.
[26] N. Klonis, N.H. Quazi, L.W. Deady, A.B. Hughes, L. Tilley, Characterization of a series of far-red-absorbing thiobarbituric acid oxonol derivatives as fluorescent probes for biological applications, Anal. Biochem. 317 (2003) 47–58, https://doi.org/10.1016/S0003-2697(03)00086-1.
[27] M. Klikar, V. Jelínková, Z. Růžičková, T. Mikysek, O. Pytela, M. Ludwig, F. Bureš, Malonic acid derivatives on duty as electron-withdrawing units in push-pull molecules, Eur. J. Org. Chem. 2017 (2017) 2764–2779, https://doi.org/10.1002/ejoc.201700070.
[28] M. Klikar, F. Bureš, O. Pytela, T. Mikysek, Z. Padělková, A. Barsella, K. Dorkenoo, S. Achelle, N, N′-Dibutylbarbituric acid as an acceptor moiety in push-pull chromophores, New J. Chem. 37 (2013) 4230–4240, https://doi.org/10.1039/c3nj00683b.
[29] A.C. Benniston, A. Harriman, K.S. Gulliya, Photophysical properties of merocyanine 540 derivatives, J. Chem. Soc. Faraday Trans. 90 (1994) 953–961, https://doi.org/10.1039/FT9949000953.
[30] S.-H. Kim, Y.-S. Kim, D.-H. Lee, Y.-A. Son, Synthesis and optical chromic properties of new barbituric acid based dye molecules having push-π-pull system, Mol. Cryst. Liq. Cryst. 550 (2011) 240–249, https://doi.org/10.1080/15421406.2011.599761.
[31] I. Bolz, C. May, S. Spange, Solvatochromic properties of Schiff bases derived from 5-aminobarbituric acid: chromophores with hydrogen bonding patterns as components for coupled structures, New J. Chem. 31 (2007) 1568–1571, https://doi.org/10.1039/B702483E.
[32] I. Bolz, C. May, S. Spange, Novel Schiff bases derived from 5-aminobarbituric acid: synthesis and solid state structure, Arkivoc. 3 (2007) 60–67.
[33] I. Bolz, C. Moon, V. Enkelmann, G. Brunklaus, S. Spange, Probing molecular recognition in the solid-state by use of an enolizable chromophoric barbituric acid, J. Org. Chem. 73 (2008) 4783–4793, https://doi.org/10.1021/jo800598z.
[34] M. Bauer, A. Rollberg, A. Barth, S. Spange, Differentiating between dipolarity and polarizability effects of solvents using the solvatochromism of barbiturate dyes, Eur. J. Org. Chem. 2008 (2008) 4475–4481, https://doi.org/10.1002/ejoc.200800355.
[35] M.L. Deb, P.J. Bhuyan, Uncatalysed Knoevenagel condensation in aqueous medium at room temperature, Tetrahedron Lett. 46 (2005) 6453–6456, https://doi.org/10.1016/j.tetlet.2005.07.111.
[36] B.S. Jursic, A simple method for knoevenagel condensation of α, β-conjugated and aromatic aldehydes with barbituric acid, J. Heterocycl. Chem. 38 (2001) 655–657, https://doi.org/10.1002/jhet.5570380318.
[37] M.J. Kamlet, J.L.M. Abboud, M.H. Abraham, R.W. Taft, Linear solvation energy relationships. 23. A comprehensive collection of the solvatochromic parameters,pi.*,alpha., and.beta., and some methods for simplifying the generalized solvatochromic equation, J. Org. Chem. 48 (1983) 2877–2887, https://doi.org/10.1021/jo00165a018.
[38] Y. Marcus, The properties of organic liquids that are relevant to their use as solvating solvents, Chem. Soc. Rev. 22 (1993) 409–416, https://doi.org/10.1039/cs9932200409.
[39] J. Shorter, Correlation Analysis in Organic Chemistry: An Introduction to Linear Free-energy Relationships, Clarendon Press, 1973.
[40] A. Williams, Free energy relationships in organic and bio-organic chemistry, Roy. Soc. Chem. (2003), https://doi.org/10.1039/9781847550927.
[41] D. Cremer, Møller-Plesset perturbation theory: from small molecule methods to methods for thousands of atoms, Wiley Interdiscip. Rev. Comput. Mol. Sci. 1 (2011) 509–530, https://doi.org/10.1002/wcms.58.
[42] A.D. Becke, Density-functional thermochemistry. III. The role of exact exchange, J. Chem. Phys. 98 (1993) 5648–5652, https://doi.org/10.1063/1.464913.
[43] C. Lee, W. Yang, R.G. Parr, Development of the Colle-Salvetti correlation-energy formula into a functional of the electron density, Phys. Rev. B. 37 (1988) 785–789, https://doi.org/10.1103/PhysRevB.37.785.
[44] M.J. Frisch, G.W. Trucks, H.B. Schlegel, G.E. Scuseria, M.A. Robb, J.R. Cheeseman, G. Scalmani, V. Barone, B. Mennucci, G.A. Petersson, Gaussian, Inc., Wallingford CT, Gaussian 09, 2009.
[45] I. Mayer, Charge, bond order and valence in the AB initio SCF theory, Chem. Phys. Lett. 97 (1983) 270–274, https://doi.org/10.1016/0009-2614(83)80005-0.
[46] Z. Liu, T. Lu, Q. Chen, An sp-hybridized all-carboatomic ring, cyclo[18]carbon: electronic structure, electronic spectrum, and optical nonlinearity, Carbon N. Y. 165 (2020) 461–467, https://doi.org/10.1016/j.carbon.2020.05.023.
[47] F. Zuccarello, G. Buemi, C. Gandolfo, A. Contino, Barbituric and thiobarbituric acids: a conformational and spectroscopic study, Spectrochim Acta Part A Mol. Biomol. Spectrosc. 59 (2003) 139–151, https://doi.org/10.1016/S1386-1425(02)00146-4.
[48] W. Bolton, The crystal structure of anhydrous barbituric acid, Acta Crystallogr. 16 (1963) 166–173, https://doi.org/10.1107/s0365110x63000438.
[49] G.A. Jeffrey, S. Ghose, J.O. Warwicker, The crystal structure of barbituric acid dihydrate, Acta Crystallogr. 14 (1961) 881–887, https://doi.org/10.1107/s0365110x61002539.
[50] A. Barakat, H.J. Al-Najjar, A.M. Al-Majid, S.M. Soliman, Y.N. Mabkhot, M.R. Shaik, H.A. Ghabbour, H.-K. Fun, Synthesis, NMR, FT-IR, X-ray structural characterization, DFT analysis and isomerism aspects of 5-(2,6-dichlorobenzylidene)pyrimidine-2,4,6(1H,3H,5H)-trione, Spectrochim Acta Part A Mol. Biomol. Spectrosc. 147 (2015) 107–116, https://doi.org/10.1016/j.saa.2015.03.016.
[51] M.C. Rezende, M. Dominguez, J.L. Wardell, J.M.S. Skakle, J.N. Low, C. Glidewell, Supramolecular structures of five 5-(arylmethylene)-1,3-dimethylpyrimidine-2,4,6(1H,3H,5H)-triones: Isolated molecules, hydrogen-bonded chains and chains of fused hydrogen-bonded rings, Acta Crystallogr. Sect. C Cryst. Struct. Commun. 61 (2005) 306–311, https://doi.org/10.1107/S0108270105008498.
[52] C.R. Groom, I.J. Bruno, M.P. Lightfoot, S.C. Ward, The Cambridge structural database, Acta Crystallogr. Sect. B. 72 (2016) 171–179, https://doi.org/10.1107/S2052520616003954.
[53] J.C. Cochran, K. Hagen, G. Paulen, Q. Shen, S. Tom, M. Traetteberg, C. Wells, On the planarity of styrene and its derivatives: the molecular structures of styrene and (Z)-$\tilde{I}^2$-bromostyrene as determined by ab initio calculations and gas-phase electron diffraction, J. Mol. Struct. 413–414 (1997) 313–326, https://doi.org/10.1016/S0022-2860(97)00071-9.
[54] J.C. Sancho-García, A.J. Pérez-Jiménez, A theoretical study of the molecular structure and torsional potential of styrene, J. Phys. B At. Mol. Opt. Phys. 35 (2002) 1509–1523, https://doi.org/10.1088/0953-4075/35/6/308.
[55] C.H. Choi, M. Kertesz, Conformational information from vibrational spectra of styrene, trans-Stilbene, and cis-Stilbene, J. Phys. Chem. A. 101 (1997) 3823–3831, https://doi.org/10.1021/jp970620v.
[56] A. Karpfen, C.H. Choi, M. Kertesz, Single-bond torsional potentials in conjugated systems: a comparison of ab initio and density functional results, J. Phys. Chem. A. 101 (1997) 7426–7433, https://doi.org/10.1021/jp971606l.
[57] T.A. Ganina, D.A. Cheshkov, V.A. Chertkov, Dynamic structure of organic compounds in solution according to NMR data and quantum chemical calculations: II. Styrene, Russ. J. Org. Chem. 53 (n.d.) 12–23. https://doi.org/10.1134/s1070428017010043.
[58] M.P. Rančić, N.P. Trišović, M.K. Milčić, I.A. Ajaj, A.D. Marinković, Experimental and theoretical study of substituent effect on 13C NMR chemical shifts of 5-arylidene-2,4-thiazolidinediones, J. Mol. Struct. 1049 (2013) 59–68, https://doi.org/10.1016/j.molstruc.2013.06.027.
[59] M.P. Rančić, I. Stojiljković, M. Milošević, N. Prlainović, M. Jovanović, M.K. Milčić, A.D. Marinković, Solvent and substituent effect on intramolecular charge transfer in 5-arylidene-3-substituted-2,4-thiazolidinediones: Experimental and theoretical study, Arab. J. Chem. 12 (2019) 5142–5161, https://doi.org/10.1016/j.arabjc.2016.12.013.

[60] Robert W. Taft, Progress in Physical Organic Chemistry, Volume 14, by John Wiley & Sons, Inc., 1983. https://doi.org/10.1002/9780470171936.
[61] W.F. Reynolds, A. Gomes, A. Maron, D.W. MacIntyre, A. Tanin, G.K. Hamer, I.R. Peat, Substituent-induced chemical shifts in 3- and 4-substituted styrenes: definition of substituent constants and determination of mechanisms of transmission of substituent effects by iterative multiple linear regression, Can. J. Chem. 61 (1983) 2376–2384, https://doi.org/10.1139/v83-412.
[62] B.A. Saleh, S.A. Al-Shawi, G.F. Fadhil, Substituent effect study on 13Cβ SCS of styrene series. A Yukawa-Tsuno model and Reynolds dual substituent parameter model investigation, J. Phys. Org. Chem. 21 (2008) 96–101, https://doi.org/10.1002/poc.1272.
[63] E. Kleinpeter, S. Klod, W.D. Rudorf, Electronic state of push-pull alkenes: An experimental dynamic NMR and theoretical ab initio MO study, J. Org. Chem. 69 (2004) 4317–4329, https://doi.org/10.1021/jo0496345.
[64] C. Reichardt, Solvents and Solvent Effects in Organic Chemistry, Wiley-VCH, Weinheim, 2003.
[65] S. Spange, N. Weiß, C.H. Schmidt, K. Schreiter, Reappraisal of empirical solvent polarity scales for organic solvents, Chem.-Methods. 1 (1) (2021) 42–60, https://doi.org/10.1002/cmtd.202000039.
[66] J. Kulhánek, F. Bureš, O. Pytela, T. Mikysek, J. Ludvík, A. Růžička, Push-pull molecules with a systematically extended π-conjugated system featuring 4,5-dicyanoimidazole, Dye. Pigment. 85 (2010) 57–65, https://doi.org/10.1016/j.dyepig.2009.10.004.
[67] L.R. Domingo, E. Chamorro, P. Pérez, Understanding the reactivity of captodative ethylenes in polar cycloaddition reactions. A theoretical study, J. Org. Chem. 73 (2008) 4615–4624, https://doi.org/10.1021/jo800572a.
[68] B. Štefane, A. Perdih, A. Pevec, T. Šolmajer, M. Kočevar, The participation of 2H-pyran-2-ones in [4+2] cycloadditions: An experimental and computational study, Eur. J. Org. Chem. (2010) 5870–5883, https://doi.org/10.1002/ejoc.201000236.
[69] S. Feng, Y.-C. Wang, Y. Ke, W. Liang, Y. Zhao, Effect of charge-transfer states on the vibrationally resolved absorption spectra and exciton dynamics in ZnPc aggregates: simulations from a non-Makovian stochastic Schrödinger equation, J. Chem. Phys. 153 (2020) 34116, https://doi.org/10.1063/5.0013935.